University of Reading

Potential volcanic impacts on future climate variability

Article

Accepted Version

Bethke, I., Outten, S., Otterå, O. H., Hawkins, E. ORCID: https://orcid.org/0000-0001-9477-3677, Wagner, S., Sigl, M. and Thorne, P. (2017) Potential volcanic impacts on future climate variability. Nature Climate Change, 7 (11). pp. 799-805. ISSN 1758-678X doi: 10.1038/nclimate3394 Available at https://centaur.reading.ac.uk/74097/

It is advisable to refer to the publisher's version if you intend to cite from the work. See Guidance on citing.
Published version at: http://dx.doi.org/10.1038/nclimate3394
To link to this article DOI: http://dx.doi.org/10.1038/nclimate3394

Publisher: Nature Publishing Group

All outputs in CentAUR are protected by Intellectual Property Rights law, including copyright law. Copyright and IPR is retained by the creators or other copyright holders. Terms and conditions for use of this material are defined in the End User Agreement.

www.reading.ac.uk/centaur

CentAUR

Central Archive at the University of Reading

Reading's research outputs online

Potential volcanic impacts on future climate variability

Ingo Bethke[1], Stephen Outten[2], Odd Helge Otterå[1], Ed Hawkins[3], Sebastian Wagner[4], Michael Sigl[5,6], Peter Thorne[7]

[1]Uni Research Climate, Bjerknes Centre for Climate Research, Bergen, Norway

[2]Nansen Environmental and Remote Sensing Center, Bjerknes Centre for Climate Research, Bergen, Norway

[3]NCAS-Climate, Department of Meteorology, University of Reading, Reading, UK

[4]Institute for Coastal Research, Helmholtz-Zentrum Geesthacht, Germany

[5]Laboratory of Environmental Chemistry, Paul Scherrer Institute, Switzerland

[6]Oeschger Centre for Climate Change Research, University of Bern, Switzerland

[7]Irish Climate Analysis and Research Units, Department of Geography, National University of Ireland Maynooth, Ireland

Corresponding author

Correspondence to: Ingo Bethke <ingo.bethke@uni.no>

New ice-core records[1] highlight large variations in volcanism over the past 2,500 years, causing variations in past climate[2]. Most state-of-the-art climate projections for the 21st century under-sample future volcanic effects by not representing the range of plausible future volcanic activity[3,4,5]. Here we explore sixty possible volcanic futures, each consistent with the ice-core records, applied to 21st century projections. Their inclusion notably enhances the climate variability on annual-to-decadal time scales. We find a 50% increase both in annual-mean global temperature variability and in decades with a negative global temperature trend. Volcanic activity also impacts probabilistic projections of global radiation, sea level, ocean circulation, and sea ice variability; and has local-scale detectible impacts. The episodic forcing only weakly affects the long-term trends and occurrence of warm years, making it unlikely to mitigate long-term global warming impacts. Conversely, the effects on variance and extremes are substantial and expected to be important for many adaptation decisions and risk assessments[6]. We thus conclude that including plausible volcanic uncertainty is both possible and important in future climate assessments.

Volcanism has been a major driver of past climate variability[2] and will continue to affect future climate alongside human influences[7]. Explosive volcanic eruptions warm the stratosphere[8], cool the troposphere[9], cause changes in the hydrological cycle[10,11], and trigger modifications of atmospheric circulation that give rise to large regional climate responses[12]. The instrumental period covering the last 150 years has been relatively volcanically quiescent, and it is therefore tempting to ascribe potential volcanism a minor role in future climate impact and risk assessments. In a millennial perspective, however, there have been periods with considerably stronger volcanic activity[1] (Supplementary Fig. 1). Clustered occurrence of strong tropical eruptions has contributed to sustained cold periods such as the Little Ice Age[13],

where the longer-term climate impacts are mediated through ocean heat content anomalies[14] and ocean circulation changes[15-17] that also affect global and regional sea level[18] and sea ice conditions[13,15].

Because volcanic eruptions are unpredictable events, they have generally been excluded from 21st century climate projection protocols. Most recent projections either specify future volcanic forcing as zero or a constant background value[5], while considerations of more realistic volcanic effects have been limited to idealised eruption scenarios, repeating recent volcanic activity in near-future simulations[3,19]. Herein we explore whether a more complete representation of volcanic forcing uncertainty that considers a range of volcanic forcing possibilities will have an impact on important aspects of probabilistic 21st century projections increasingly being used for adaptation planning purposes. The risk from not realistically accounting for volcanic forcing effects is that critical possible future outcomes are being discounted and mal-adaptation ensues.

The possibility of utilizing stochastic volcanic forcing in projections has been recognised in previous studies[20] and underscored in the latest assessment report of the Intergovernmental Panel on Climate Change[21]. Increasing computational power facilitating large ensemble simulations[22], together with improved reconstructions of past volcanic activity[1] that allow for a better statistical characterisation[7,20], make it timely to revisit the question of volcanic effects on 21st century climate projections. We start by deriving plausible future volcanic forcings (Fig. 1) by sampling from reconstructed volcanic activity of the last 2,500 years[1] (Supplementary Fig. 1). We next perform three 21st century simulation ensembles with the Norwegian Earth System Model (NorESM)[23], that use the same mid-range anthropogenic forcing scenario RCP4.5[24] but differ in their volcanic forcing: a 60-member ensemble using plausible stochastic volcanic forcing (VOLC); a 60-member reference ensemble using zero volcanic forcing (NO-VOLC); and a 20-member ensemble using 1850–2000 averaged volcanic forcing[25] (VOLC-CONST). NO-VOLC and VOLC-CONST are the two approaches that were adopted across the group of models contributing 21st century projections to the Coupled Model Intercomparison Project phase 5 (CMIP5)[26]. Hence we consider both as useful counterfactual cases here to aid reader interpretation of possible limitations in existing 21st century projection runs. Specifically, we assessed the volcanic influence on the climate variability and means of future projections by comparing our three ensembles for several societally relevant diagnostics.

We start by examining the impact of future volcanic activity on Global-Mean Surface Air Temperature (GMST) – an integrated climate change indicator of particular relevance to mitigation decision making. Figure 2a shows annual-mean GMST changes over the course of the 21st century as simulated in the three ensembles. The effect of volcanic forcing on the ensemble mean temperature (thick solid lines) is modest, amounting to a 5% reduction of the

centennial GMST change projected under RCP4.5, with VOLC and VOLC-CONST being slightly cooler than NO-VOLC throughout the post-2005 period as expected from the first-order response to volcanic forcing. Near-term GMST projections for the 2016–2035 period (Fig. 2b) exhibit only a small (0.05 K) reduction in mean response in VOLC and VOLC-CONST, with an increased skew in VOLC leading to a 0.1 K shift in the lower distribution tail. As a result, the 1.5ºC warming target of the Paris agreement COP-21[22] is exceeded on average two years later in VOLC and VOLC-CONST (Supplementary Table 1), with the upper distribution tail of VOLC being shifted by twice that amount (Fig. 2c). Models which did not include constant background forcing in their standard 21st century simulations prepared for CMIP5 are thus overly-pessimistic as to the likely time until different warming thresholds are reached.

Over the course of the simulation period, the ensemble mean difference grows, eventually saturating just below 0.1 K around 2040 (Fig. 2a), after which the means are well separated. The delay highlights the role of slow-response components, particularly the ocean[14,15], in aggregating the global response to episodic volcanic forcing. The general correspondence of the VOLC and VOLC-CONST ensemble shows that the application of a time-invariant background forcing adequately accounts for long-term aspects of volcanic impacts in the ensemble mean projections. One could use plausible low and high background values To further account for projection uncertainty stemming from uncertainty in the centennial-mean volcanic forcing, (Fig. 1c and Supplementary Fig. 1). However, this would fail to capture the response to episodic volcanic forcing and attendant impacts on annual-to-decadal variability and extremes.

The interannual uncertainty range (5-95% ensemble spread) in annual-mean GMST is inflated by more than 50% (from 0.3 to 0.5 K) in VOLC relative to NO-VOLC (Fig. 2a – red vs blue shading; individual VOLC ensemble member GMST are shown in Supplementary Fig. 9). Consistent with a tropospheric cooling response, the change in ensemble spread in VOLC relative to NO-VOLC is skewed towards lower GMST, leaving the higher bound largely unaltered (Fig. 2d). Reductions in frequency of extremely warm years are generally small, whereas increases in frequency of extremely cold years – relative to the moving average or 'present-day' climate at any point – are much more substantial. In contrast, the application of a constant background forcing merely shifts the distribution of VOLC-CONST relative to NO-VOLC, overestimating the reduction of warm years and underestimating the increase of cold years.

Decadal-scale GMST series are even more affected by future volcanic forcing uncertainty than annual temperatures (Fig. 3a). The distribution of the decadal means – with the global warming trend removed prior to the analysis – is considerably wider for VOLC than for NO-VOLC, with roughly a doubling in standard-deviation (Fig. 3b and Supplementary Table 1). Anomalously cold decades become more frequent at the expense of 'normal' and, to a lesser degree, anomalously warm decades. As for decadal means, the spread in decadal trends is significantly wider for VOLC than for NO-VOLC (Fig. 3c). Occurrences of decades with negative GMST trend become more frequent if accounting for volcanic forcing, with the probability increasing from 10% in NO-VOLC to more than 16% in VOLC (Fig. 3d). Conversely, the widening of the upper tail of the decadal trend distribution (Fig. 3c) indicates enhanced probability of decadal-scale warming surges, due to the rebound of GMST after volcanic induced cooling has reached its maximum (cf. Supplementary Fig. 4). The probability of decades with negative GMST trend more than doubles from 4% to 10% (Fig.

3e) if the analysis is limited to the first half of the century – before the stabilization period of RCP4.5 – suggesting that the relative impact is sensitive to other forcings and depends on the anthropogenic scenario. Volcanic induced cooling becomes increasingly important in facilitating neutral or negative temperature trends on longer timescales on which natural internal variability effects such as ENSO are no longer sufficient to offset anthropogenic forcings (Fig. 3f,g).

That volcanic influence is not limited to GMST projections becomes evident from assessing selected global and large-scale climate indicators that all have previously been found to be sensitive to volcanism[11,15-18] (Fig. 4 and Supplementary Table 1). The radiative forcing at the top of the atmosphere is reduced by 0.05 W/m^2 on average (Fig. 4a), while its decadal standard-deviation, including the anthropogenic RCP4.5 signal, is increased by 80% in response to volcanic forcing. The distribution of decadal radiative anomalies is widened with a skew towards lower values (Fig. 4b) and a slight occurrence of more positive extremes resulting from reduced radiative surface cooling in post-eruption years. Global sea level rise is on average slowed by 4% (relative to RCP4.5) in VOLC compared to NO-VOLC (Fig. 4c) as a direct consequence of reduced heat uptake by the oceans. The distribution of decadal sea level anomalies is significantly widened (doubling of standard-deviation after subtracting global warming trend) with the lower uncertainty tail being affected most (Fig. 4d). Contrary to GMST, the volcanic forcing is generally not strong enough to halt global steric sea level rise by offsetting anthropogenic driven ocean warming on decadal and longer time scales. Asian summer monsoon precipitation shows consistent, albeit small reductions (Fig. 4e), with all decades featuring lower ensemble means, and a 20% overall increase in ensemble standard-deviation (Fig. 4f). The Atlantic Meridional Overturning Circulation (AMOC) evaluated at 26ºN shows a relative strengthening of 0.2 Sv in VOLC compared to NO-VOLC

(Fig. 4g), with all decades exhibiting increased ensemble means, and a 20% overall increase in ensemble standard-deviation (Fig. 4h). Similarly, Arctic sea ice volume shows a 1-2% relative increase for most decades (Fig. 4i) and a 15% increase in ensemble standard-deviation (Fig. 4j), with more overlap between the spread of subsequent decades in VOLC compared to NO-VOLC indicating enhanced probability for a temporary halt in Arctic sea ice decline.

To address if the inclusion of volcanic forcing variability has local implications we performed a time-of-emergence (ToE) analysis[27] on seasonally averaged surface air temperature (Fig. 5). The ToE is formally defined as the mean time at which the signal of climate change emerges from the noise of natural climate variability (see Methods). The simulated impact of volcanic forcing variability on the ToE changes is distinct but small. The ToE is delayed almost everywhere as a consequence of the inclusion of volcanic forcing (Fig. 5a,b). The distribution of the simulated delay is strongly skewed and indicates a ToE delay of up to a decade in some locations, and of three years on average (Fig. 5c,d).

Our results highlight the importance of representing volcanic forcing uncertainty in probabilistic future climate projections, in particular for risk assessments with focus on variability and certain extremes. Counter to earlier findings of destructive interference of volcanic forcing with internal climate variability modes[16], our stochastic volcanic forcing generally amplifies the annual-to-decadal scale climate variability in our model. A sharp increase in simulated decades with negative GMST trend exemplifies the effect of volcanic forcing uncertainty on projections of climate extremes. While volcanic-induced GMST trends have arguably limited direct human impacts, similar effects on other extremes – such as Arctic sea ice extent or reduced monsoon precipitation – lead to direct socioeconomic

consequences. Extreme volcanic activity can potentially cause extended anomalously cold periods. This will, however, not help to mitigate long-term global warming impacts as the surface climate is likely to rebound, leaving its long-term trajectory virtually unaltered (Fig. 2a, yellow curve).

This study is a first step towards incorporating current knowledge on global volcanic activity in probabilistic future climate projections in realistic and systematic ways. It serves as a proof-of-concept for a statistical representation of potential volcanism in 21st century climate projections and demonstrates the importance of such a representation for the projections of future climate variability. Our ensemble analysis, based on a single model and a single anthropogenic scenario, provides only a conditional assessment of the volcanic contribution to climate projection uncertainty[28]. Additional uncertainties in the volcanic forcing reconstruction, in other external forcings and in the model (details in Supplementary Information) warrant further experiments. Since simulated regional impacts are less distinct than global impacts and have larger model uncertainty[28], quantifying volcanic impacts on regional climate projections and their socio-economic aspects should be a priority of future work. Improved characterisation of past volcanic forcing, improved representation of volcanic impact in models, and coordinated multi-model efforts using the same plausible forcings are essential ingredients for advancing the utilisation of volcanism information in future climate assessments. The newly established Model Intercomparison Project on climatic response to Volcanic forcing (VolMIP)[29] presents the ideal platform for integrating these efforts.

References

1. Sigl, M. *et al.* Timing and climate forcing of volcanic eruptions for the past 2,500 years. *Nature* **523,** 543–549 (2015).
2. Schurer, A. P., Tett, S. F. B. & Hegerl, G. C. Small influence of solar variability on climate over the past millennium. *Nat. Geosci.* **7,** 104–108 (2014).
3. Hansen, J. et al. Global climate changes as forecast by Goddard Institute for Space Studies three-dimensional model. *J. Geophys. Res.* **93**, 9341 (1988).
4. Gregory, J. M. Long-term effect of volcanic forcing on ocean heat content. *Geophys. Res. Lett.* **37** (2010).
5. O'Neill, B. C. *et al.* The Scenario Model Intercomparison Project (ScenarioMIP) for CMIP6. *Geosci. Model Dev.* **9,** 3461–3482 (2016).
6. Oppenheimer, C. Climatic, environmental and human consequences of the largest known historic eruption: Tambora volcano (Indonesia) 1815. *Prog. Phys. Geogr.* **27,** 230–259 (2003).
7. Hyde, W. T. & Crowley, T. J. Probability of Future Climatically Significant Volcanic Eruptions. *J. Clim.* **13,** 1445–1450 (2000).
8. Parker, D. E. & Brownscombe, J. L. Stratospheric warming following the El Chichón volcanic eruption. *Nature* **301,** 406–408 (1983).
9. Robock, A. & Mao, J. The Volcanic Signal in Surface Temperature Observations. *J. Clim.* **8,** 1086–1103 (1995).
10. Iles, C. E. & Hegerl, G. C. Systematic change in global patterns of streamflow following volcanic eruptions. *Nat. Geosci.* **8,** 838–842 (2015).
11. Liu, F. *et al.* Global monsoon precipitation responses to large volcanic eruptions. *Sci. Rep.* **6,** 24331 (2016).

12. Shindell, D. T., Schmidt, G. A., Mann, M. E. & Faluvegi, G. Dynamic winter climate response to large tropical volcanic eruptions since 1600. *J. Geophys. Res* **109,** D05104 (2004).

13. Miller, G. H. *et al.* Abrupt onset of the Little Ice Age triggered by volcanism and sustained by sea-ice/ocean feedbacks. *Geophys. Res. Lett.* **39** (2012).

14. Gleckler, P. J. *et al.* Volcanoes and climate: Krakatoa's signature persists in the ocean. *Nature* **439,** 675 (2006).

15. Stenchikov, G. et al. Volcanic signals in oceans. *J. Geophys. Res.* **114,** D16104 (2009).

16. Swingedouw, D. *et al.* Bidecadal North Atlantic ocean circulation variability controlled by timing of volcanic eruptions. *Nat. Commun.* **6,** 6545 (2015).

17. Otterå, O. H., Bentsen, M., Drange, H. & Suo, L. External forcing as a metronome for Atlantic multidecadal variability. *Nat. Geosci.* **3,** 688–694 (2010).

18. Church, J. A., White, N. J. & Arblaster, J. M. Significant decadal-scale impact of volcanic eruptions on sea level and ocean heat content. *Nature* **438,** 74–7 (2005).

19. Shiogama, H. *et al.* Possible Influence of Volcanic Activity on the Decadal Potential Predictability of the Natural Variability in Near-Term Climate Predictions. *Adv. Meteorol.* **2010,** 1–7 (2010).

20. Ammann, C. M. & Naveau, P. A statistical volcanic forcing scenario generator for climate simulations. *J. Geophys. Res.* **115,** D05107 (2010).

21. Kirtman, B., S.B. Power, J.A. Adedoyin, G.J. Boer, R. Bojariu, I. Camilloni, F.J. Doblas-Reyes, A.M. Fiore, M. Kimoto, G.A. Meehl, M. Prather, A. Sarr, C. Schar, R. Sutton, G.J. van Oldenborgh, G. Vecchi and H.J. Wang, 2013: Near-term Climate Change: Projections and Predictability. In: *Climate Change 2013: The Physical Science Basis. Contribution of Working Group I to the Fifth Assessment Report of the Intergovernmental Panel on Climate Change*

22. Mitchell, D. *et al.* Realizing the impacts of a 1.5 °C warmer world. *Nat. Clim. Chang.* **6,** 735–737 (2016).

23. Bentsen, M. *et al.* The Norwegian Earth System Model, NorESM1-M – Part 1: Description and basic evaluation of the physical climate. *Geosci. Model Dev.* **6,** 687–720 (2013).

24. Vuuren, D. P. *et al.* The representative concentration pathways: an overview. *Clim. Change* **109,** 5–31 (2011).

25. Ammann, C. M., Meehl, G. A., Washington, W. M. & Zender, C. S. A monthly and latitudinally varying volcanic forcing dataset in simulations of 20th century climate. *Geophys. Res. Lett.* **30,** 1657 (2003).

26. Taylor, K. E. *et al.* An Overview of CMIP5 and the Experiment Design. *Bull. Am. Meteorol. Soc.* **93,** 485–498 (2012).

27. Hawkins, E. & Sutton, R. Time of emergence of climate signals. *Geophys. Res. Lett.* **39** (2012).

28. Hawkins, E. & Sutton, R. The Potential to Narrow Uncertainty in Regional Climate Predictions. *Bull. Am. Meteorol. Soc.* **90,** 1095–1107 (2009).

29. Zanchettin, D. *et al.* The Model Intercomparison Project on the climatic response to Volcanic forcing (VolMIP): experimental design and forcing input data for CMIP6. *Geosci. Model Dev.* **9,** 2701–2719 (2016).

Online Methods

Historical volcanic data utilised.

We consider multiple ice-cores from Greenland and Antarctica utilising the sulphate contained in the ice-core as a proxy for explosive volcanic activity of the past 2,500 years[1].

Although the approach is subject to uncertainties arising from issues such as: dating uncertainties; scaling of sulphate peaks to changes in stratospheric aerosol loads; representativeness of different regions over Greenland and Antarctica for volcanic sulphate emissions; and discrimination of single tropical versus two individual high latitude eruptions, it provides an insight into the plausible range of magnitude and temporal structure of future volcanic eruptions. Ice-core records, however, do omit small volcanic events which may nevertheless have some impacts on climate[30]. Earlier reconstructions[31-33] of past volcanic eruptions for the last millennium AD show similar temporal evolution and timing, albeit with differences in magnitude. The use of multiple cores in our reconstruction is thought to improve on earlier overestimates of, in particular, larger eruptions[34] such as the Samalas eruption in 1257[35]. The series represents the longest currently available annually-resolved continuous series, making it particularly suitable for our study. The series provides information on timing, magnitude of sulphur injection and location (tropical versus extratropical in respective hemisphere) of a total of 283 eruption events for which ice-core sulphate concentrations exceeded a detection threshold (approximately 1/3 of the strength of a tropical eruption such as Pinatubo in 1991) defined by the natural variability of non-volcanic sulphate in the ice. Eruptions from Iceland and Alaska are expected to be overrepresented in this dataset due to their proximity to Greenland. Anthropogenic SO_2 emissions predominantly from the United States and Europe peaking in the 1970-1980s (i.e., 'global dimming'[36]) mask volcanic sulphate contributions in Greenland ice cores during parts of the 20th century[37], hampering detection and quantification of volcanic sulphate deposition for eruptions such as El Chichón in 1982. Nevertheless, that the last 150 years were comparatively 'quiet' is supported by the ice-cores from Antarctica, which are not subject to significant human sulphate pollution and suggest that the stratospheric loadings between 1850–2000 CE were 30% lower compared to the 1–2000 CE average[34].

Stochastic forcing generation.

We generated plausible future eruption chronologies by resampling the past volcanic activity described in the prior section (code in Supplementary Information). For each month of the period 2006 to 2099, we draw random numbers from a uniform distribution to test whether one or more of the 283 eruption events in Sigl et al.[1] were triggered in that ensemble member on that date. For the test we assumed a constant eruption probability of 1/(2500*12), which is the probability of randomly picking the exact month from the 2,500 year record when a specific eruption event occurred. By repeating this procedure for all months and all forcing members, we obtained 60 unique plausible future eruption chronologies for the 21st century (using the CMIP5 standard period 2006–2099), with statistics that resemble those of the historical reconstruction (Supplementary Fig. 2).

We then translated the plausible 21st century eruption chronologies into model forcing ancillaries. First, we estimated peak stratospheric sulphate aerosol loadings by scaling the ice-core depositions of the individual events using established scaling relations[31]. The peak loadings were then used to scale the generic dispersal evolution of volcanic aerosols – one generic evolution for tropical and one for extratropical eruptions (Supplementary Fig. 6) – that are applied in the model[25]. We validated this approach by comparing ice-core based historical forcing, that we constructed in the same way, to the model's default historical forcing (see section 2 in Supplementary Information for details). The comparison reveals no systematic bias, and a time-mean difference of less than 10% (Supplementary Fig. 7).

Implementation and validation of volcanic forcing.

The ice-core based reconstruction of Sigl et al.[1] provides global estimates for maximum stratospheric volcanic aerosol load following the volcanic eruptions and whether the eruptions were tropical or NH/SH extratropical. To translate this information into model forcing, we analysed the data set of Ammann et al.[25] who used a transport model to estimate the spatio-temporal dispersal of stratospheric volcanic aerosols for the 20th century. We found that their dispersal evolution can be approximated by three shape functions (Supplementary Fig. 6) - one for tropical and two for extratropical NH/SH eruptions - that only depend on pressure, latitude and time since eruption start. We derived the final model forcing by scaling the shape functions with the maximum aerosol load estimated from the ice-core reconstruction. Our forcing implementation thus does not consider the seasonal effects on dispersal of volcanic aerosols discussed in Ammann et al.[25].

We compare the volcanic forcing that we generated from the ice-core data with the Ammann et al.[25] forcing for the period 1850–2000 in order to assess whether our model forcing is biased towards low or high values (Supplementary Fig. 7). While the timing and forcing magnitudes match well for some eruptions (e.g., 1883–Krakatau, 1963–Agung and 1991–Mt. Pinatubo), they differ for others (e.g., 1902–Santa Maria, 1980–Mt. St. Helens and 1982–El Chichón) partly for reasons previously outlined. Despite discrepancies for individual eruptions, however, no systematic differences in size or frequency distributions are seen and the time-means – 1.15 Tg versus 1.22 Tg volcanic aerosol lead in ice-core based versus Ammann et al.[25] forcing – match well.

Model configuration.

We performed all simulations with the medium resolution configuration of the Norwegian Earth System Model version 1 (NorESM1-M)[23,38], a state-of-the-art climate model that

provided input to the fifth Coupled Model Intercomparison Project (CMIP5)[26]. We used the exact configuration that was employed in performing those CMIP5 runs. NorESM1-M is based on the Community Climate System Model version 4[39]. Important modifications to the latter are the employment of an isopycnic coordinate ocean component, improving the conservation and transformation properties of water masses, and the addition of a more advanced aerosol-cloud chemistry treatment in the atmosphere component. The land and sea ice components are adopted in their original form.

The atmosphere and land components are configured on a regular 1.9°x2.5° horizontal grid, while the ocean and sea-ice components are configured on a 1° curvilinear horizontal grid with the northern pole singularity shifted over Greenland. The atmospheric component features 26 hybrid sigma-pressure levels extending to 3 hPa. The ocean component features a stack of 51 isopycnic layers, with a variable depth bulk mixed-layer on top.

NorESM1-M has been used to study the effect of major extratropical eruptions[40,41], where volcanic sulphur dioxide was directly injected into the atmosphere and subsequent oxidation to sulphate aerosols was simulated by the model. This approach is not applicable here as it would require a statistical model for sulphur emissions that can provide exact geographic locations, injection rates as well as injection heights. Hence, we prescribe volcanic sulphate aerosol concentrations, following the approach used for NorESM's CMIP5 simulations[23], where the model reads a mass distribution of stratospheric volcanic sulphate aerosols (Supplementary Fig. 6), which is converted to number concentrations – assuming a fixed, log-normal size distribution – and combined with prognostic sulphate before being passed to the radiation code.

Model spin-up and sensitivity test.

We generated starting conditions for the 21st century simulations by performing a 26-year spinup experiment, which we spawned off three simulation sets with 20 members each from the year 1980 states of NorESM's three historical CMIP5 simulations[23]. Initial spread within each set was generated through adding small ($O(10^{-6}K)$) noise to the ocean mixed layer temperatures. The total of 60 members were integrated to the end of year 2005, after which time the ensemble spread had reached saturation on most relevant diagnostics[42,43], such as AMOC variability (Supplementary Fig. 8). As a result, the covariability between individual members of our 21st century simulations is very close to zero.

We performed a 60-member spin-up ensemble for the post-Mt. Pinatubo eruption period 1990–2005, that is identical to the first one but with the forcing of the Mt. Pinatubo eruption removed. Analysing the differences of the two ensembles allowed us to verify the model's sensitivity to volcanic forcing (details in Supplementary Information).

Bootstrap confidence intervals.

We used empirical bootstrapping[44] to assess statistical robustness. For each test, we generated 10,000 bootstrap samples by resampling the original data with replacement. We then performed our analysis on each bootstrap sample and derived 5-95% confidence intervals by ranking the results. In the generation of the bootstrap sample, we treated the data from individual simulations as contiguous blocks[45] in order to account for effects of autocorrelation along the temporal dimension. The autocorrelation along the ensemble dimension was zero by construction.

Pre-industrial (PI) reference climate.

We show all diagnostics relative to a pre-industrial reference climate to put the volcanic impacts into a climate change perspective. We computed the reference climatology from the 500-year-long pre-industrial control simulation that NorESM contributed to CMIP5[23,26]. This simulation used external forcings fixed at 1850 levels and no volcanic forcing.

Time-of-Emergence (ToE) analysis.

Our ToE analysis on seasonally averaged surface air temperature follows Hawkins & Sutton[27]. We define ToE as the earliest occurrence where the signal-to-noise ratio exceeds the value 2 (climate change signal is distinguishable from zero at a 95% confidence level). For each simulation member, we estimated the signal by regressing the local time series onto the corresponding global mean time series. We then estimated the noise, i.e., unforced internal climate variability, from standard-deviations of a 500 year-long pre-industrial control simulation[23] that was run with the same model configuration as used in this study. The obtained ToEs were averaged over the respective NO-VOLC and VOLC ensemble. The analysis was performed for extended boreal winter (October-March) and boreal summer (April-September) averages.

Code availability.

The code for the generation of synthetic volcanic forcings is included in the Supplementary Information. The Norwegian Earth System Model can be obtained by sending a request to noresm-ncc@met.no.

Data availability.

The model output from this study and volcanic forcing ancillaries are available at https://doi.org/10.11582/2017.00006

References

30. Santer, B. D. *et al.* Volcanic contribution to decadal changes in tropospheric temperature. *Nat. Geosci.* **7,** 185–189 (2014).
31. Gao, C., Oman, L., Robock, A. & Stenchikov, G. L. Atmospheric volcanic loading derived from bipolar ice cores: Accounting for the spatial distribution of volcanic deposition. *J. Geophys. Res.* **112,** D09109 (2007).
32. Crowley, T. J. & Unterman, M. B. Technical details concerning development of a 1200 yr proxy index for global volcanism. *Earth Syst. Sci. Data* **5,** 187–197 (2013).
33. Sigl, M. *et al.* A new bipolar ice core record of volcanism from WAIS Divide and NEEM and implications for climate forcing of the last 2000 years. *J. Geophys. Res. Atmos.* **118,** 1151–1169 (2013).
34. Sigl, M. *et al.* Insights from Antarctica on volcanic forcing during the Common Era. *Nat. Clim. Chang.* **4,** 6–10 (2014).
35. Vidal, C. M. *et al.* The 1257 Samalas eruption (Lombok, Indonesia): the single greatest stratospheric gas release of the Common Era. *Sci. Rep.* **6,** 34868 (2016).
36. Wild, M. *et al.* From Dimming to Brightening: Decadal Changes in Solar Radiation at Earth's Surface. *Science.* **308,** 847–850 (2005).
37. McConnell, J. R. *et al.* 20th-Century Industrial Black Carbon Emissions Altered Arctic Climate Forcing. *Science.* **317,** 1381–1384 (2007).
38. Iversen, T. *et al.* The Norwegian Earth System Model, NorESM1-M – Part 2: Climate response and scenario projections. *Geosci. Model Dev.* **6,** 389–415 (2013).
39. Gent, P. R. *et al.* The Community Climate System Model Version 4. *J. Clim.* **24,** 4973–4991 (2011).

40. Pausata, F. S. R., Grini, A., Caballero, R., Hannachi, A. & Seland, Ø. High-latitude volcanic eruptions in the Norwegian Earth System Model: the effect of different initial conditions and of the ensemble size. *Tellus B* **67** (2015).

41. Pausata, F. S. R., Chafik, L., Caballero, R. & Battisti, D. S. Impacts of high-latitude volcanic eruptions on ENSO and AMOC. *Proc. Natl. Acad. Sci.* **112** (2015).

42. Outten, S., Thorne, P., Bethke, I. & Seland, Ø. Investigating the recent apparent hiatus in surface temperature increases: 1. Construction of two 30-member Earth System Model ensembles. *J. Geophys. Res. Atmos.* **120,** 8575–8596 (2015).

43. Thorne, P., Outten, S., Bethke, I. & Seland, Ø. Investigating the recent apparent hiatus in surface temperature increases: 2. Comparison of model ensembles to observational estimates. *J. Geophys. Res. Atmos.* **120,** 8597–8620 (2015).

44. Efron, B. & Tibshirani, R. Bootstrap Methods for Standard Errors, Confidence Intervals, and Other Measures of Statistical Accuracy. *Stat. Sci.* **1,** 54–75 (1986).

45. Carlstein, E. The Use of Subseries Values for Estimating the Variance of a General Statistic from a Stationary Sequence. *Ann. Stat.* **14,** 1171–1179 (1986).

Figures

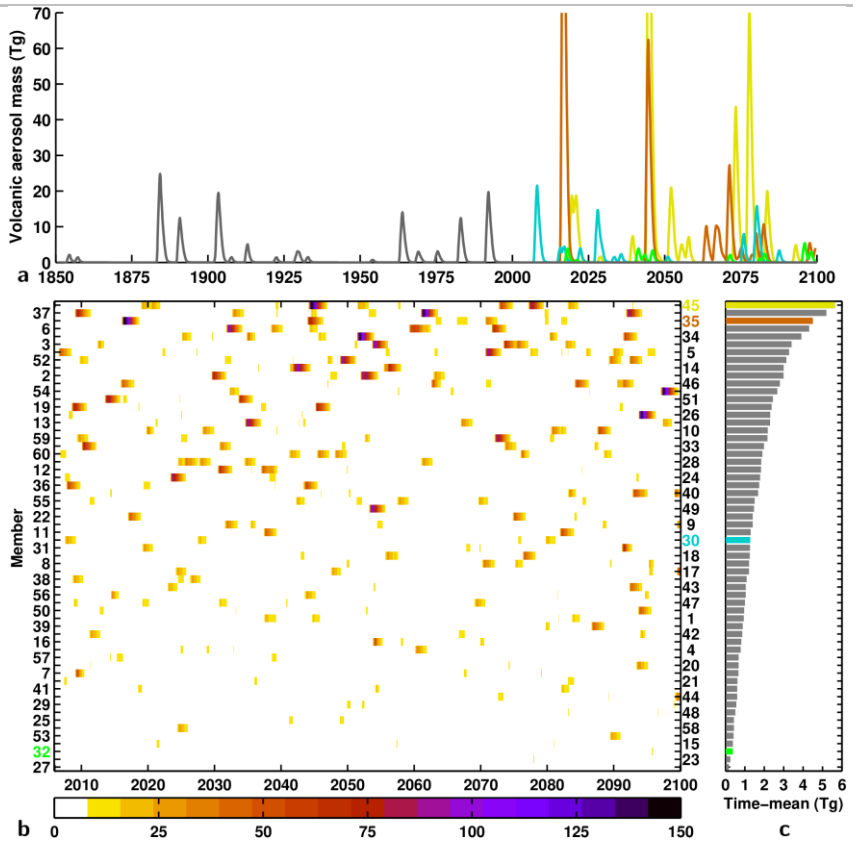

Fig. 1 | **Historical and plausible future volcanic forcing**. **a,** Stratospheric volcanic aerosol loadings in the model's historical and 21st century CMIP5 simulations[23,25] (grey) and synthetic forcing realisations with statistically low (5%, green), mid (50%, magenta), high (95%, brown) and extreme (>98%, yellow) loadings when compared to the historical reconstructions over the past 2,500 years[1]. The data are monthly, filtered with a 12-month running mean. **b,** Stratospheric aerosol loading time series and **c,** their century means for all simulation members. Members are ranked according to their time-mean loadings. Colour marked realisations correspond to the three realisations displayed in panel **a**.

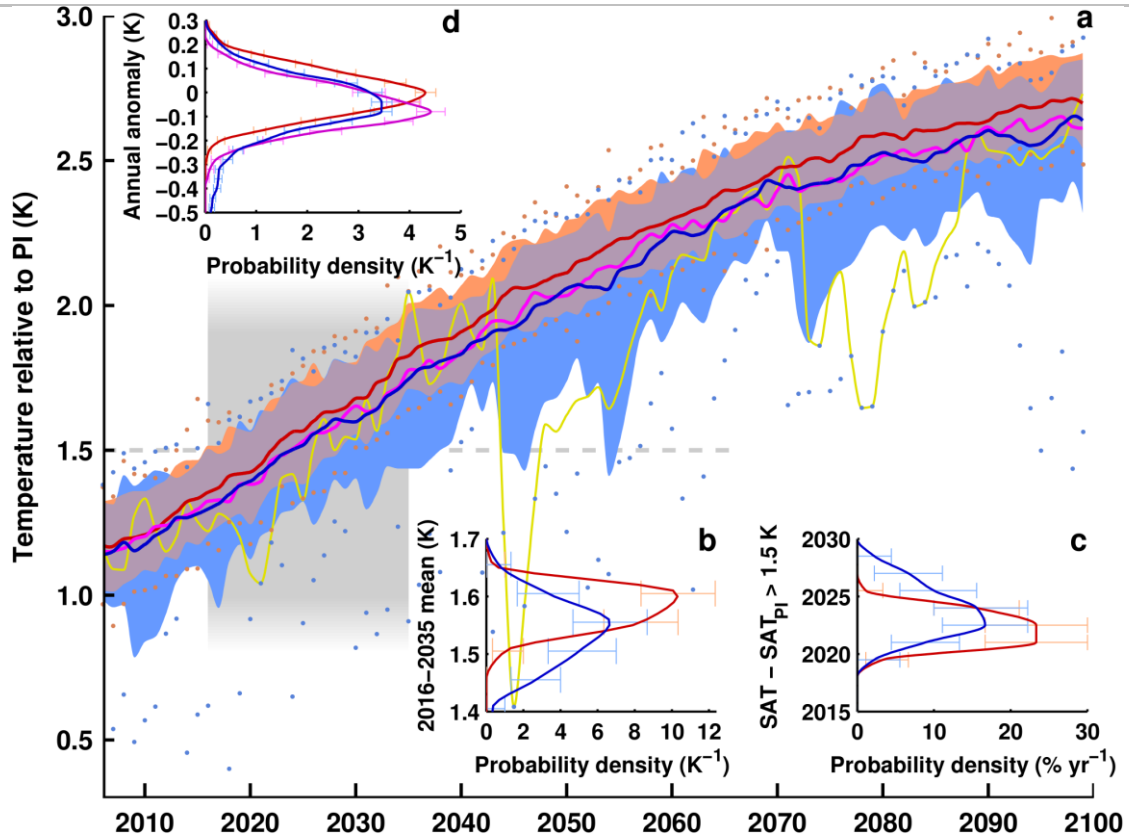

Fig. 2 | **Annual-mean GMST. a,** Ensemble mean (solid) of VOLC (blue), VOLC-CONST (magenta) and NO-VOLC (red) with 5-95% range (shading) and ensemble minima/maxima (dots) for VOLC and NO-VOLC; evolution of the most extreme member (yellow). **b,** Probability density function (PDF) of the 2016-2035 mean relative to pre-industrial (PI, see Methods), with 5-95% bootstrap confidence bounds. **c,** PDF of the time when SAT change relative to PI (20 year running average) exceeds 1.5 K. **d,** PDF of annual anomalies with anthropogenic trend removed. The spread of VOLC-CONST is linearly shifted relative to NO-VOLC and therefore not shown in **a**, **b** and **c**.

465

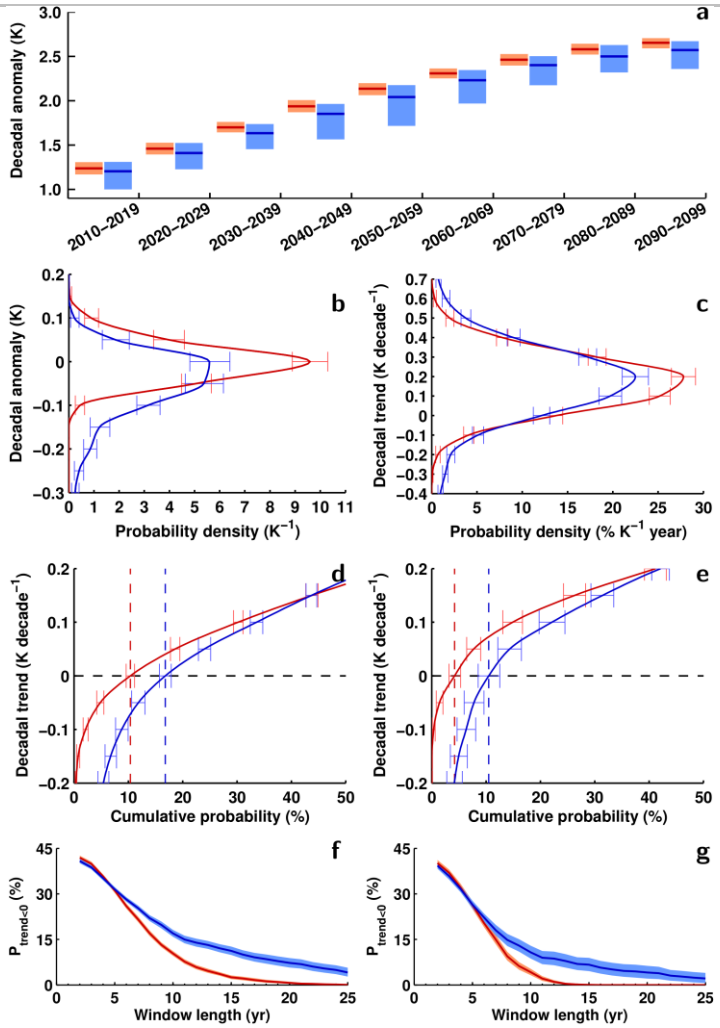

Fig. 3 | **Decadal temperature means and trends. a,** Decadal means of GMST relative to pre-industrial. Ensemble mean (solid) with 5-95% range (shading) of VOLC (blue) and NO-VOLC (red). **b,** PDF with 5-95% bootstrap confidence bounds of decadal anomalies (without overlap) relative to NO-VOLC ensemble mean. **c,** As **b,** but for decadal trends. **d,** Cumulative probability distribution with 5-95% confidence bounds for decadal trends (with overlap), using a 10-year window that is moved over 2006–2099. **f,** Probability for obtaining negative trends as function of length (solid) with 5-95% bootstrap confidence bounds (shading). **e,g,** As **d,f,** but for the shorter period 2006–2050.

466

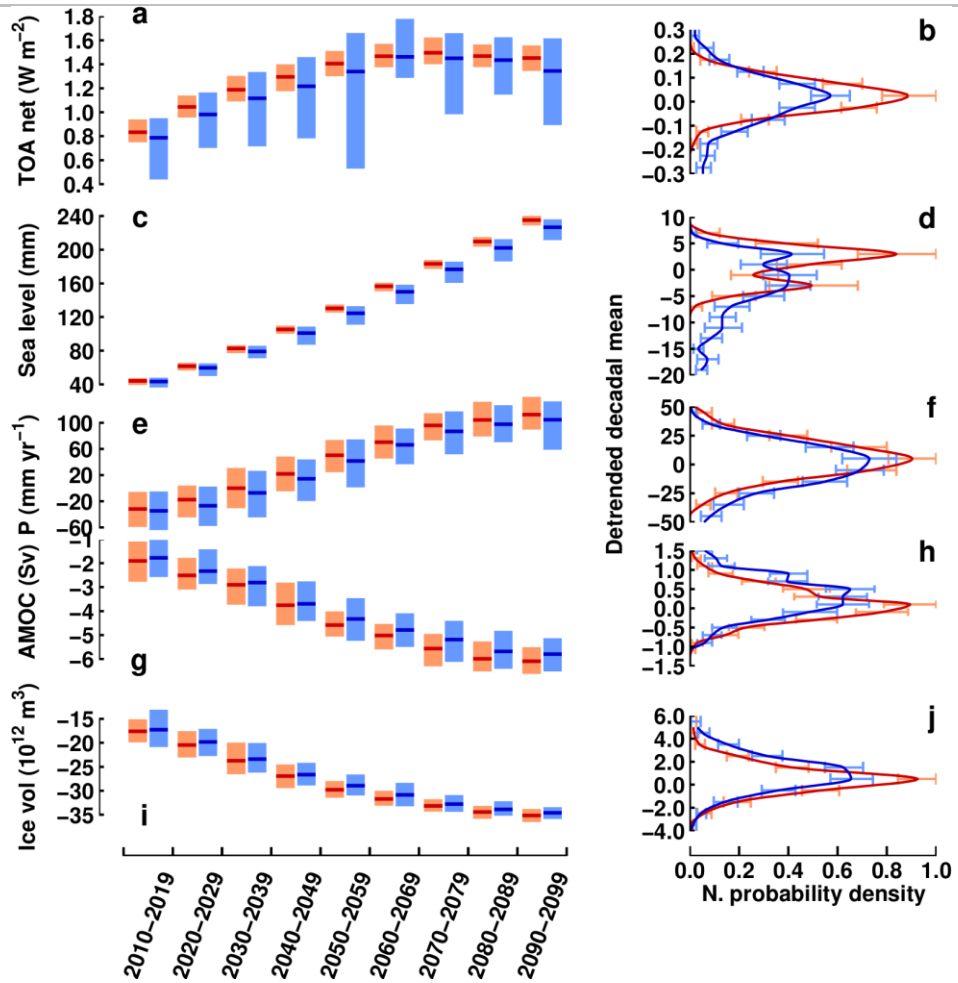

Fig. 4 | **Decadal means of large-scale climate indicators. a,** Top-of-atmosphere net radiation balance. **c,** Global steric sea level. **e,** May–September precipitation, averaged over Asian continent box [60-135ºE, 5-55ºN] (see Supplementary Fig. 5). **g,** Atlantic Meridional Overturning Circulation (AMOC) strength at 26ºN. **i,** Northern Hemisphere sea ice volume. Ensemble mean relative to pre-industrial (solid) of VOLC (blue) and NO-VOLC (red) with 5-95% range (shading). **b,d,f,h,j,** PDFs, normalized by maximum value and NO-VOLC ensemble mean subtracted prior to computation, with 5-95 bootstrap confidence bounds. The results of VOLC-CONST are shifted relative to NO-VOLC but otherwise similar and therefore not shown.

467

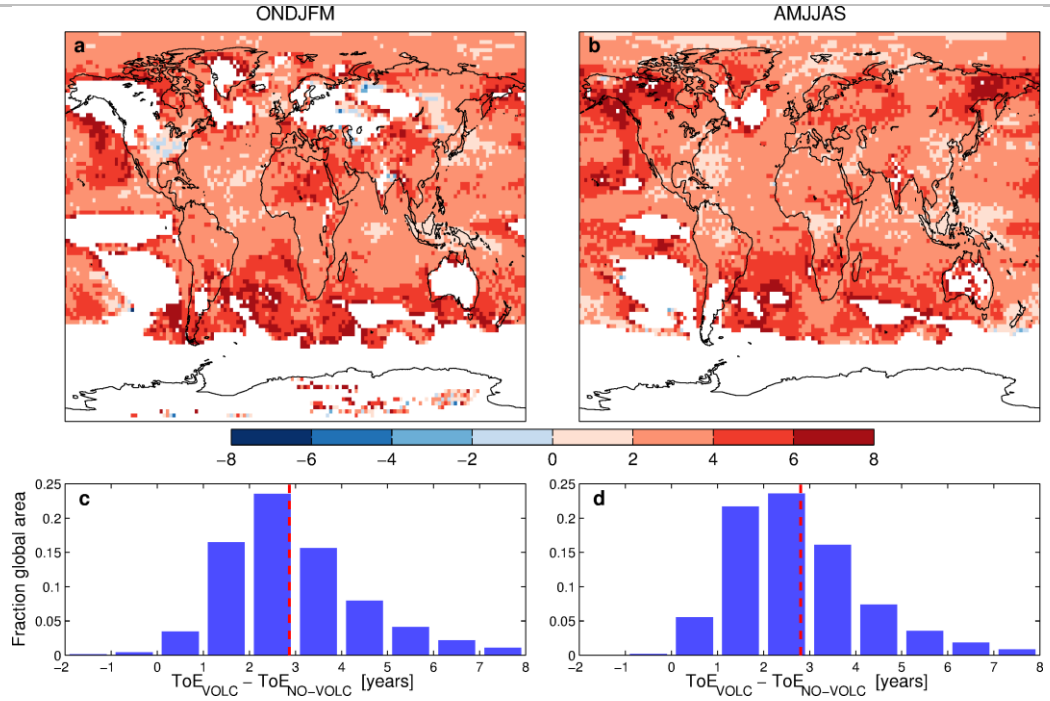

Fig. 5 | **Time of emergence of anthropogenic GMST changes.** VOLC – NO-VOLC difference in ToE relative to 1985–2005 mean for **a,** boreal winter and **b,** boreal summer, in years. Regions with no apparent emergence before 2100 are shaded in grey. **c,d,** Areal distribution of ToE differences. Dashed line denotes the weighted global mean. Only regions that show emergence between 2006 and 2099 in both ensembles are considered.

468

Acknowledgements

We thank XXX. This study was funded by YYY.

Individual author contributions

S.O., P.T. and I.B. developed the stochastic forcing model. S.W. and M.S. helped with the utilisation and interpretation of the ice-core reconstructions. I.B., P.T., S.O. and E.H. conceived and designed the simulation experiments. E.H. performed the ToE analysis. All authors contributed to writing the manuscript.